



FUCCI sensors: powerful new tools for analysis of cell proliferation

N. Zielke and B. A. Edgar*

Visualizing the cell cycle behavior of individual cells within living organisms can facilitate the understanding of developmental processes such as pattern formation, morphogenesis, cell differentiation, growth, cell migration, and cell death. Fluorescence Ubiquitin Cell Cycle Indicator (FUCCI) technology offers an accurate, versatile, and universally applicable means of achieving this end. In recent years, the FUCCI system has been adapted to several model systems including flies, fish, mice, and plants, making this technology available to a wide range of researchers for studies of diverse biological problems. Moreover, a broad range of FUCCI-expressing cell lines originating from diverse cell types have been generated, hence enabling the design of advanced studies that combine *in vivo* experiments and cell-based methods such as high-content screening. Although only a short time has passed since its introduction, the FUCCI technology has already provided fundamental insight into how cells establish quiescence and how G1 phase length impacts the balance between pluripotency and stem cell differentiation. Further discoveries using the FUCCI technology are sure to come.

© 2015 The Authors. *WIREs Developmental Biology* published by Wiley Periodicals, Inc.

How to cite this article:

WIREs Dev Biol 2015, 4:469–487. doi: 10.1002/wdev.189

INTRODUCTION

In recent decades, intense research and numerous fundamental discoveries have led to a relatively detailed knowledge of the regulatory network that governs the eukaryotic cell cycle.¹ Most of these groundbreaking studies were conducted in unicellular organisms or immortalized cultured cells that proliferate autonomously when supplied with sufficient nutrients and growth factors. But in most situations in animals and plants, whether a cell proliferates, remains dormant, or exits the cell cycle to differentiate depends largely on its interactions with neighboring cells and physiological signals from elsewhere in the organism. Thus to tackle general problems in development, regeneration, and the transformation of normal cells

into tumor cells, it is essential to understand how cell proliferation is regulated by a cell's context.

Analysis of proliferating cells in whole organisms has proven difficult because traditional cell cycle markers such as nucleotide analogs (BrdU, EdU), or replication proteins (PCNA, Ki-67) rely on immunofluorescent detection, which requires sample fixation. Recently, a novel methodology was introduced that allows monitoring cell cycle phasing in living cells, named FUCCI (Fluorescent Ubiquitination-based Cell Cycle Indicator).² Since its introduction in 2008, the FUCCI technology has revolutionized the analysis of cell proliferation *in vivo* and thereby permitted a number of groundbreaking discoveries (Figure 1). The FUCCI system takes advantage of two components of the DNA replication control system of higher eukaryotes, the licensing factor Cdt1 and its inhibitor Geminin. Cdt1 and Geminin have opposing effects on DNA replication, their abundance oscillates during the cell cycle, in an inverse pattern.³ Cdt1 protein peaks in G1 phase just before the onset of DNA replication, and declines abruptly after the initiation of S phase.^{4,5} In

*Correspondence to: b.edgar@zmbh.uni-heidelberg.de

Deutsches Krebsforschungszentrum (DKFZ), Zentrum für Molekulare Biologie der Universität Heidelberg (ZMBH) Allianz, Heidelberg, Germany

Conflict of interest: The authors have declared no conflicts of interest for this article.

opposition, Geminin levels are high during S and G2 phase, but low during late mitosis and G1 phase.⁶ The reciprocal expression of Cdt1 and Geminin is affected by the sequential activation of the E3 ubiquitin ligases APC/C^{Cdh1} and SCF^{Skp2}. The APC/C ubiquitin ligase is active from mid-mitosis throughout G1 and targets Geminin for degradation, whereas the SCF^{Skp2} ubiquitin ligase is active only during S and G2 phases and targets Cdt1 for degradation.³ Interestingly, SCF^{Skp2} is a substrate of APC/C^{Cdh1}, a condition that enforces their reciprocally timed activity.^{7,8} The FUCCI system relies on pairs of fluorescent proteins fused to degrons derived from Cdt1 and Geminin. These fluorescent FUCCI 'probes' are destabilized by APC/C and SCF^{Skp2} during different phases of the cell cycle, and thereby allow the accurate visualization of living cells in either G1 or S/G2/M by virtue of which FUCCI probe they express (Figure 2(a)).² It is important to note that although most FUCCI systems are based on dual probes, it is possible to determine the cell cycle stage with a single FUCCI probe. The use of both probes, however, produces more reliable results because the cell continuously alternates between green and red, permitting automatic detection and continuous tracking of migrating cells.

The first iteration of the G1 sensor included the complete human Cdt1 protein fused to a monomeric version of Kusabira Orange (mKO2).² However, ectopic expression of this construct interfered with cell cycle progression. This prompted Sakaue-Sawano and coworkers to engineer a chimeric protein that supports normal cell cycle progression but still oscillates normally. The human Cdt1 protein contains three functional domains (Figure 2(c)): the N-terminal region harbors a PIP box, which is recognized by the S phase-specific ubiquitin ligase CRL4^{Cdt2}.^{9,10} The PIP box is followed by another degron termed Cy motif, which is crucial for proteasomal targeting by the SCF^{Skp2} ubiquitin ligase.^{9,10} The central part of Cdt1 mediates the interaction with Geminin, whereas the C-terminal domain is crucial for the loading of minichromosome maintenance (MCM) proteins.^{4,11–15} The authors generated various deletion constructs and discovered that an N-terminal fragment of hCdt1 (hCdt1_{30–120}) is sufficient for degradation during S and G2 phase. This truncation eliminates the Geminin-binding region but maintains the Cy motif (aa 68–70), which is critical for SCF^{Skp2}-mediated proteasomal degradation.¹⁰ The deletion of the PIP box appeared to be crucial for the generation of a functional G1 sensor,² but in retrospect this is a surprising finding as FUCCI sensors in most other species are solely based on the PIP box motif. Another noteworthy observation is that this

original G1 sensor is only functional in conjunction with mKO2 or mCherry, whereas fusions with the monomeric version of AzamiGreen (mAG), EGFP, or mRFP1 were constantly expressed throughout the cell cycle (Figure 2(e)).^{2,16}

The human Geminin protein, used for the S/G2/M sensor, also contains several conserved domains (Figure 2(b)): The N-terminal portion of Geminin harbors a destruction (D) box (RRTLKVIQP) that is crucial for APC/C-mediated degradation,^{6,17} and the central portion contains a coiled-coil domain that mediates Cdt1 binding.^{15,18,19} Nuclear targeting of Geminin relies on two clusters of Arg and Lys residues that are localized between the D box and the coiled-coil domain.^{17,20} Based on this information, Sakaue-Sawano et al. engineered a fusion protein consisting of mKO2 and the N-terminal region of hGem (mAG-hGem_{1–110}) that allows robust detection of S/G2/M phase.

The original FUCCI probes were both localized in the nucleus, which has many advantages, but also some disadvantages. On the one hand, nuclear targeting facilitates the detection of the reporter probes; but on the other hand, it makes it nearly impossible to recognize cell types and differentiation states based on characteristic cell morphologies. To overcome this limitation, Sakaue-Sawano and coworkers extended their engineering approach, which gave rise to an even shorter Geminin fragment (hGem_{1–60}) that is evenly distributed throughout the cell because it lacks a KKAK motif that is crucial for effective nuclear localization.^{20,21} It turned out to be impossible to create an evenly distributed Cdt1 fragment that accumulates specifically during G1 phase, but this is only a minor drawback because in combination with hGem_{1–60} the silhouette of a cell can be recognized through most of the cell cycle. In contrast to hCdt1_{30–120}, both hGem_{1–110} and hGem_{1–60} support normal cell cycle oscillations in combination with various fluorescent proteins such as mAG, mCyan, Venus, or mCherry (Figure 2(e)).^{16,21,22} The increased selection of fluorochromes supports the design of complex experimental setups involving multiple fluorescent reporter constructs, enabling the researcher to correlate cell cycle progression with various cellular processes such as protein subcellular localization or signaling events.

FUCCI EXPRESSING MICE

A major advantage of genetically encoded biosensors is that they allow the generation of transgenic organisms that can be used in various experimental setups and thus provide valuable resources for the

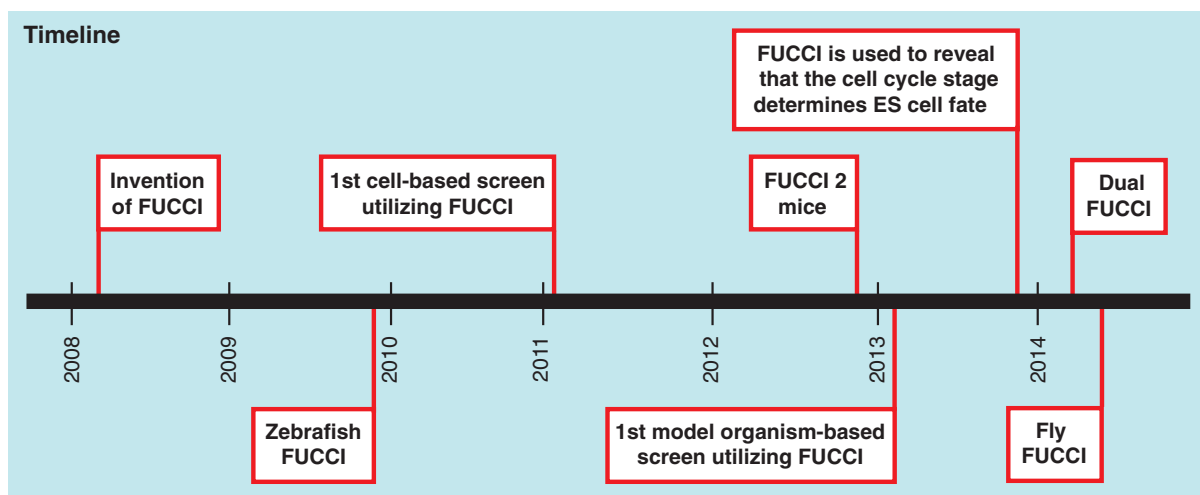


FIGURE 1 | Timeline illustrating the invention of the different FUCCI variants and the key discoveries that have been made with them.

research community (Table 1). Therefore, the team of Atsushi Miyawaki has generated transgenic mice that express either mKO2-hCdt1₃₀₋₁₂₀ or mAG-hGem₁₋₁₁₀ under control of the synthetic CAG promoter, which includes the cytomegalovirus (CMV) early enhancer element and promoter, the first exon and first intron of the chicken β -actin gene, and the splice acceptor of the rabbit β -globin gene.³⁷ To obtain *bona fide* FUCCI mice, the lines CAG-mKO2-hCdt1₃₀₋₁₂₀ (#596) and CAG-mAG-hGem₁₋₁₁₀ (#504) were crossbred and further characterized. FUCCI#596/#504 transgenic mice showed red or green fluorescence expression in many somatic cell types (Table 1). As a proof of principle, the expression pattern of the FUCCI probes was determined in the developing brain using live microscopy.² In the developing cerebral cortex, certain neural progenitors exit the cell cycle and migrate beyond the ventricular zone, where they differentiate into neurons or, at later stages, into glial cells. Tracking of FUCCI-expressing cells revealed that cells shift during migration from G1 to S/G2/M phase, demonstrating that the FUCCI method is suited for the analysis of cell cycle oscillations in complex tissues. A recent study showed that FUCCI#596/#504 mice have strong expression in the heart, which led to the development of an *ex vivo* culturing system to analyze cardiomyocyte proliferation by live microscopy.³⁸ This approach indicated that the duration of S/G2/M phases increases during development, implying a link between the cell cycle and cardiomyocyte differentiation. Although the FUCCI probes used in the FUCCI#596/#504 mice are broadly expressed, the probes are not detectable in hematopoietic organs like spleen and bone marrow. However, random integration of expression constructs results in multiple lines

with variable characteristics and two other combinations of FUCCI probes, CAG-mKO2-hCdt1₃₀₋₁₂₀ (#639) and CAG-mAG-hGem₁₋₁₁₀ (#492), and CAG-mKO2-hCdt1₃₀₋₁₂₀ (#610) and CAG-mAG-hGem₁₋₁₁₀ (#474) support robust expression in spleen and bone marrow.^{22,24,25} The FUCCI#639/#492 mice have been used to identify quiescent (G1-arrested) IgG1-type memory B cells in the spleen and to visualize their proliferation (activation) upon secondary immunization.²⁵

A major drawback of the first generation of FUCCI mice is that the corresponding transgenes are localized on different chromosomes, which complicated the maintenance of the line. To overcome this problem, Abe et al. generated a new transgenic line, named R26p-FUCCI 2, which expresses both FUCCI sensors bidirectionally from a single transgene.²⁶ Besides easier maintenance, the new design has the advantage that it simplifies the crossing of the FUCCI sensors into diverse mutant backgrounds. Instead of mKO2 and mAG, the FUCCI 2 mice use mCherry-hCdt1₃₀₋₁₂₀ and mVenus-hGem₁₋₁₁₀ (Figure 3(b)). These sensors produce better color contrast and can be spectrally separated from GFP.¹⁶ Another problem of the first generation FUCCI mice is that the probes are expressed at very low levels in certain tissues. This variability is likely caused by the random integration of the FUCCI probes such that the CAG promoter is inactive or only weakly active in several tissues.^{39,40} To solve the latter problem, the CAG promoter was replaced by the ubiquitously active Rosa26 promoter (R26p).⁴¹ To avoid positional effects of the transgene integration site, the R26p-FUCCI 2 construct was flanked by chicken hypersensitive site 4 (cHS4) insulator sequences.^{42,43} cHS4 insulator sequences were also

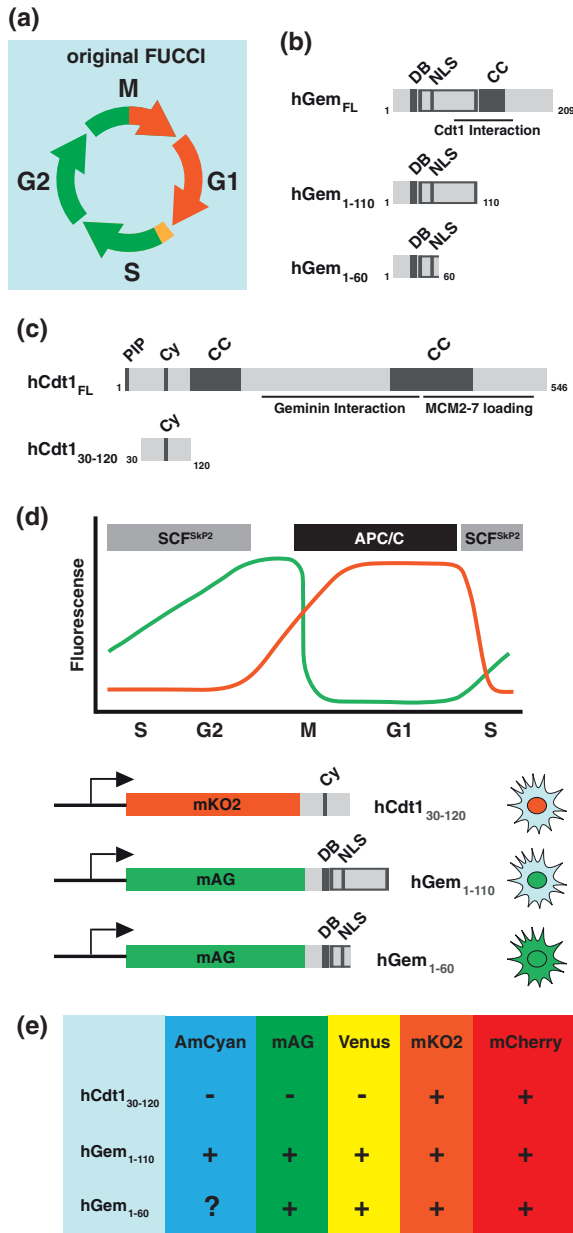


FIGURE 2 | The FUCCI concept. (a) The original FUCCI sensors mark cells residing in G1 phase with red fluorescence, while cells in S/G2/M are labeled in green. During a short period at the G1/S transition, both probes are present and hence the cells appear yellow. (b) Domain structure of the human Geminin-based S/G2/M sensors. DB, destruction box; NLS, nuclear localization signal; CC, coiled-coil domain. (c) Domain structure of the human Cdt1-based G1 sensor. PIP, PCNA interaction motif; Cy, Cy motif; CC, coiled-coil domain. (d) Time plot illustrating the sequential degradation of the FUCCI probes. Nuclear mAG-hGem₁₋₁₁₀ or pan-localized mAG-hGem₁₋₆₀ accumulates during S and G2 phase, but is targeted for degraded during late mitosis and G1 phase by the E3 ligase, APC/C. The nuclear mKO-hCdt1₃₀₋₁₂₀ probe accumulates during G1 phase and is degraded during S and G2 phase by the SCF^{SKP2} complex. (e) Overview of the fluorescent proteins that produce functional FUCCI sensors.

utilized to separate the bidirectionally expressed FUCCI probes. Although the R26p-FUCCI 2 line can be maintained only in a heterozygous state, this line showed robust expression of the FUCCI probes in embryonic tissues such as blastomeres at early cleavage stages as well as in extra-embryonic tissues. Consistent with an earlier study in cell culture,¹⁶ the mCherry-hCdt1₃₀₋₁₂₀ signal is detectable throughout G1 phase, but diminishes upon entry into S phase. In contrast, the mVenus-hGem₁₋₁₁₀ signal is present during S and G2 phases, and disappears rapidly in late M phase. Because both mCherry-hCdt1₃₀₋₁₂₀ and mVenus-hGem₁₋₁₁₀ are absent during late M phase, no fluorescence signal was detected during that period. Conversely, there was a short period at the transition from G1 to S phase during which the cells emitted both red and yellow fluorescence.

As mentioned above, the first generation of FUCCI mice suffered from variable expression levels of the probes due to the positional effects of random transgenesis. To completely avoid artifacts resulting random integration, another set of FUCCI mice (Figure 3(c)–(e)) was generated in which the probes were integrated into the Rosa26 locus via gene targeting, named R26R-FUCCI 2. The Rosa26 locus supports ubiquitous gene expression, and its disruption has no apparent side effects.^{44–47} To support the tracing of cell cycle oscillation in a tissue- or cell type-specific manner, either mCherry-hCdt1₃₀₋₁₂₀ or mVenus-hGem₁₋₁₁₀ were combined with a loxP-flanked stop cassette that can be removed by the expression of Cre recombinase.⁴⁸ A large collection of mice strains expressing Cre recombinase under control of defined enhancer sequences now exists, to which R26R-FUCCI 2 mice can be crossed, providing a means for tissue-specific expression of the FUCCI sensors. Both R26R-mCherry-hCdt1₃₀₋₁₂₀ and R26R-mVenus-hGem₁₋₁₁₀ mice are homozygous viable and exhibit no apparent defects. To characterize the R26R-FUCCI 2 mice, both lines were crossed with the EIIa-Cre line that is based on the adenovirus EIIa promoter and targets the expression of the Cre recombinase to the early mouse embryo.⁴⁹ Both sensors were readily detectable during early embryogenesis and displayed characteristic cell cycle oscillations. The brightness of R26R-mVenus-hGem₁₋₁₁₀ was similar to the R26R-FUCCI 2 mice, but the signal of mCherry was reduced to about a half. One drawback of the R26R lines is that, as only one FUCCI sensor is employed, the fluorescence signal is lost during half of the cell cycle. This complicates the tracking of individual cells, which can be ‘lost’ during their long dark phase. However, this problem can be overcome by combining the R26R mice with constitutive cellular

TABLE 1 | Transgenic FUCCI Animals

Mice				
Name	FUCCI Probe(s)	Promoter	Notes	References
<i>Mouse (Mus musculus)</i>				
FUCCI-S/G2/M#504	mAG-hGem ₁₋₁₁₀	CAG	Constant expression in most tissues, except hematopoietic system	2, 23
FUCCI-S/G2/M#492	mAG-hGem ₁₋₁₁₀	CAG	Constant expression in the spleen	24, 25
FUCCI-S/G2/M#474	mAG-hGem ₁₋₁₁₀	CAG	Constant expression in the bone marrow, high-level expression in B lymphoid cells	22, 24
R26R-Venus-hGem ₁₋₁₁₀	Venus-hGem ₁₋₁₁₀	Knock-in in <i>rosa26</i> locus	Conditional expression with Cre/LoxP system. Homozygous viable, no apparent defects	26
FUCCI-G1#596	mKO2-hCdt1 ₃₀₋₁₂₀	CAG	Constant expression in most tissues, except hematopoietic organ	2, 27
FUCCI-G1#639	mKO2-hCdt1 ₃₀₋₁₂₀	CAG	Constant expression in the spleen	24, 25
FUCCI-G1#610	mKO2-hCdt1 ₃₀₋₁₂₀	CAG	Constant expression in the bone marrow	22, 24
R26R-mCherry-hCdt1 ₃₀₋₁₂₀	mCherry-hCdt1 ₃₀₋₁₂₀	Knock-in in <i>rosa26</i> locus	Conditional expression with Cre/LoxP system. Homozygous viable, no apparent defects	26
R26P-FUCCI 2	mCherry-hCdt1 ₃₀₋₁₂₀ and Venus-hGem ₁₋₁₁₀	Rosa26 (R26P)	Can only be maintained in a heterozygous state, robust expression in embryonic and extra-embryonic tissues	26
R26-FUCCI 2aR	mCherry-hCdt1 ₃₀₋₁₂₀ -T2A-Venus-hGem ₁₋₁₁₀	CAG, reverse knock-in in <i>rosa26</i> locus	Strong ubiquitous expression at all examined time points including trunk, forelimbs lung, and kidney at E13. Homozygous viable	28
<i>Zebrafish (Danio rerio)</i>				
Ceycil	mKO2-zCdt1 ₁₋₁₉₀ and mAG-zGem ₁₋₁₀₀	EF1 α	Constant expression during early development	29
Ceycil2	mKO2-zCdt1 ₁₋₁₉₀ and mAG-zGem ₁₋₆₀	EF1 α	Constant expression during early development	29
C1mc2:zFUCCI	mCherry-zCdt1 ₁₋₁₉₀ and Venus-hGem ₁₋₁₁₀	Cardiac myosin light chain 2 (<i>cmlc2</i>)	Specifically expressed in embryonic caridomyocytes	30
Ins:zFUCCI	mCherry-zCdt1 ₁₋₁₉₀ and mAG-zGem ₁₋₁₀₀	Insulin regulatory element	Specifically expressed in pancreatic β -cells	31, 32
Dual FUCCI	Cherry-zCdt1 ₁₋₁₉₀ and Flag-Cerulean-zGem ₁₋₁₀₀	Ubiquitin (pUb)	Constant expression during all developmental stages and in adult fish	33, 34
<i>Fruitfly (Drosophila melanogaster)</i>				
S/G2/M-Green	mAG-hGem ₁₋₁₁₀	UAS _t	Bipartite expression systems allows specific labeling of cells in S/G2 and M phases in almost every tissue	35
Fly-FUCCI	GFP-dE2F1 ₁₋₂₃₀ and mRFP1-dCycB ₁₋₂₆₆	Ubiquitin (pUb), UAS _t , UAS _p , QUAS	Constant expression in most cell types with pUb, bipartite expression systems allow specific expression almost every tissue	36
	CFP-dE2F1 ₁₋₂₃₀ and Venus-dCycB ₁₋₂₆₆	UAS _t , UAS _p , QUAS	Bipartite expression systems allow specific expression almost every tissue	36
	GFP-dE2F1 ₁₋₂₃₀ and mRFP1-NLS-dCycB ₁₋₂₆₆	Ubiquitin (pUb), UAS _t , UAS _p , QUAS	Constant expression in most cell types with pUb, bipartite expression systems allow specific expression almost every tissue, NIS-CycB ₁₋₂₆₆ is not functional polyploid tissues	36
	CFP-dE2F1 ₁₋₂₃₀ and Venus-NLS-dCycB ₁₋₂₆₆	UAS _t , UAS _p , QUAS	Bipartite expression systems allow specific expression almost every tissue, NIS-CycB ₁₋₂₆₆ is not functional polyploid tissues	36

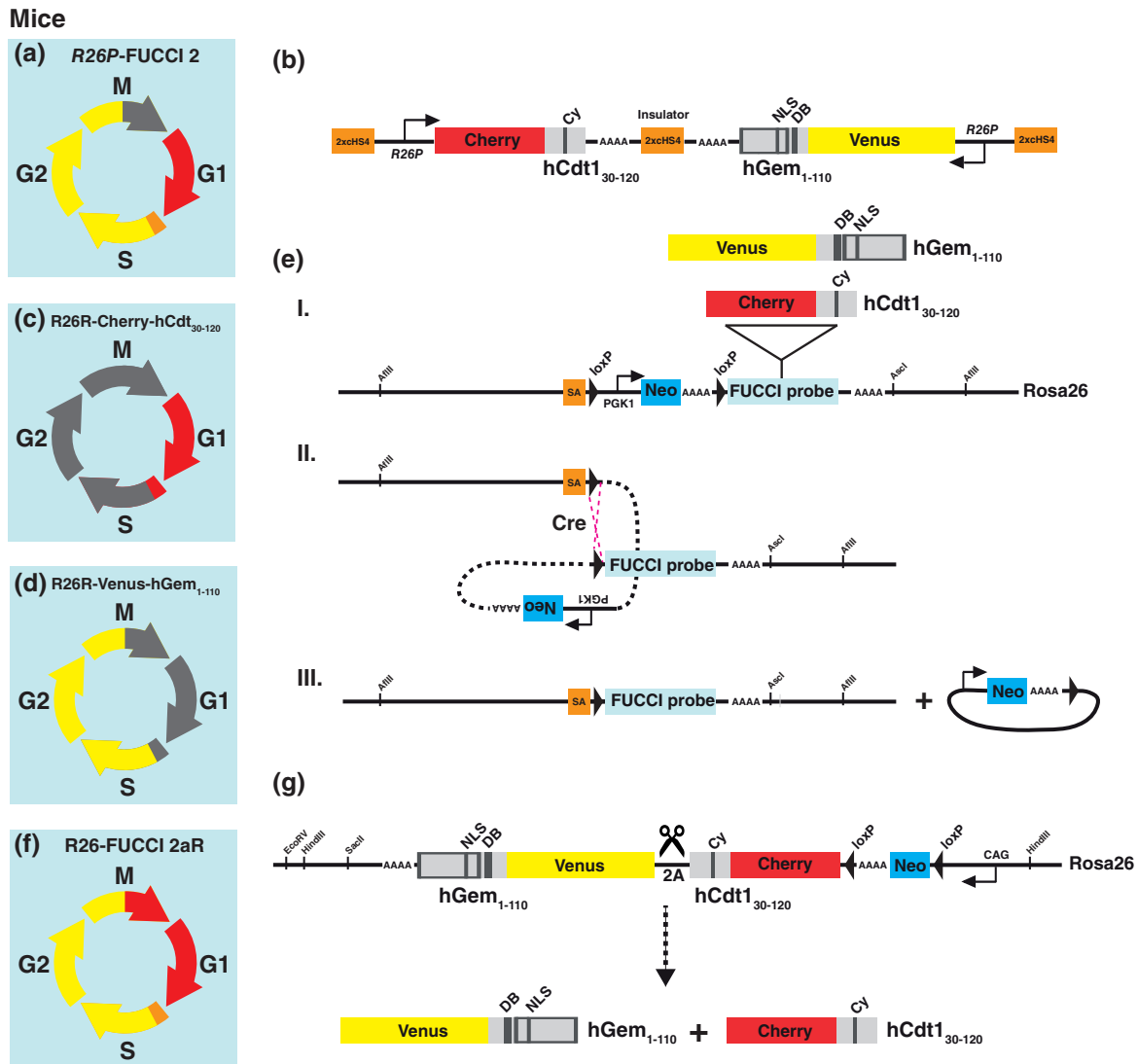


FIGURE 3 | Fucci-expressing mice. (a) In R26P-FUCCI 2 mice, G1 cells are constitutively labeled by red fluorescence, whereas cells in S and G2 phases are marked in yellow. (b) Diagram of the R26P-FUCCI 2 expression construct. mCherry-hCdt1₃₀₋₁₂₀ and mVenus-hGem₁₋₁₁₀ are bidirectionally expressed from the ubiquitous rosa26 promoter (R26p). Two copies of the chSC4 insulator separate the individual components of the R26P-FUCCI 2 construct. (c) R26R-mCherry-hCdt1₃₀₋₁₂₀ mice conditionally mark cells in G1 phase by red fluorescence. (d) R26R-mVenus-hGem₁₋₁₁₀ mice conditionally label cells in S/G2 phase by yellow fluorescence. (e) Either mCherry-hCdt1₃₀₋₁₂₀ or mVenus-hGem₁₋₁₁₀ was targeted to the rosa26 locus. To control the expressions of mCherry-hCdt1₃₀₋₁₂₀ or mVenus-hGem₁₋₁₁₀ in time and space, a neo cassette (neomycin-resistant gene expressed under the control of the PGK1 promoter) flanked by loxP sequences was placed in front of each probe. The neo cassette can be excised by Cre-mediated loxP recombination, resulting in expression of the Fucci probes in all Cre-expressing cells. SA, adenovirus splice acceptor. (g) R26R-FUCCI2aR mice conditionally mark cells in G1 phase by red fluorescence and cells S/G2 phase by yellow fluorescence. (f) The multicistron Fucci2aR construct was inserted in reverse orientation into the Rosa26 locus. The targeting construct contains the CAG promoter, a stop cassette consisting of the neomycin resistance gene flanked by loxP sites, mCherry-hCdt1₃₀₋₁₂₀ and mVenus-hGem₁₋₁₁₀. Both Fucci probes are separated by a 2A auto-cleavage site, which produces iso-stoichiometric quantities of both Fucci probes.

markers such as H2B-EGFP or H2B-mCherry.^{48,50} These shortcomings, however, have motivated the development of another new Fucci line termed R26-FUCCI 2aR, which enables conditional expression of both Fucci probes.²⁸ In the R26-FUCCI 2aR line, mCherry-hCdt1₃₀₋₁₂₀ and mVenus-hGem₁₋₁₁₀ as well as a Cre-removable stop cassette have been

targeted in reverse orientation to the rosa26 locus (Figure 3(g)). Instead of the endogenous promoter, the R26-FUCCI 2aR design relies on the synthetic CAG promoter, which yields higher expression than the endogenous promoter. One key feature of the R26-FUCCI 2aR design is that the two Fucci probes are separated by a 2A sequence, which

catalyzes the separation of the individual peptides by a co-translational mechanism termed ribosome skipping.⁵¹ This design has the advantage that both probes are always expressed in the same ratio, which simplifies the detection of green–red transitions. Moreover, the streamlined design of the R26-FUCCI2aR line facilitates the combination of the FUCCI sensors with mutant backgrounds or other transgenic lines. As a proof of principle, Mort et al. have analyzed the expression in the developing lung epithelium of FUCCI2aR mice, and discovered remarkable regional differences in cell cycle phasing.²⁸ Actively branching regions were predominantly in S/G2/M phase, whereas the prospective bronchial regions were mostly comprised of cells residing in G1 phase.

FUCCI-EXPRESSING CELL LINES

The FUCCI technology is widely applicable in cell biology and therefore it is not surprising that several FUCCI-expressing cell lines have been developed (Table 2). The most obvious application of these cell lines is to use the FUCCI sensors as a means for determining whether a certain treatment alters the duration of specific cell cycle phases. For example, a recent study used FUCCI-expressing human retinal pigment epithelial (RPE-1) cells to demonstrate that depletion of a centrosomal protein (CEP164) decreases the overall length of the cell cycle, but prolongs S phase.⁶⁹ CEP164 has been implicated in nephronophthisis, an autosomal recessive polycystic kidney disease that is caused by dysfunction of the primary cilia, and thus these data may provide a link between aberrant DNA replication and the pathogenesis of nephronophthisis. Another recent study used FUCCI-expressing HeLa cells to demonstrate that chemical inhibition of atypical protein kinase C (aPKC) impedes cell proliferation by lengthening G1 and S phases.⁷⁰ Further experiments revealed that aPKC impinges on the cyclin-dependent kinase inhibitor (CKI) p27/Xic1, which is a major determinant of G1 length. Together with functional studies conducted in *Xenopus* embryos, these data provide a direct link between apical–basal polarity and cell cycle progression, which may explain why polarized neural stem cells prefer proliferation to differentiation.

The FUCCI sensors can also serve as an effective means for connecting cellular processes such as protein degradation or changes in subcellular localization to specific stages of the cell cycle. Santos et al. utilized the FUCCI sensors to determine the cell cycle stages at which nuclear targeting of CycB1 induces mitosis.⁷¹ Likewise, Son et al. utilized FUCCI-expressing mouse lymphoblasts to

measure the rate of cellular growth in each cell cycle stage.⁶⁵ This analysis revealed a distinct change in the growth rate at the G1–S transition, implying that growth and cell cycle progression are interconnected. Moreover, FUCCI-expressing non-transformed, immortalized RPE-1 cells were successfully used to study the impact of DNA damage on cell fate decisions. This work revealed that non-transformed cells progressively lose the capacity to restore cell proliferation after DNA damage-induced G2 arrest, forcing them to undergo senescence. G1 cells, by contrast, retained their ability to reenter the cell cycle after DNA damage.⁵² A parallel study demonstrated that different phosphatases mediate the reversal of checkpoint arrest in G1 or G2.⁵³ Although WT p53-induced phosphatase 1 (Wip1) is crucial for the recovery in G2-arrested cells by antagonizing p53, it appears to be dispensable for the recovery of G1-arrested cells. Further experiments revealed that phosphoprotein phosphatase 4 catalytic subunit (PP4) mediates cell cycle re-entry after DNA damage in G1. PP4 dephosphorylates Krüppel-associated box domain-associated protein-1 (Kap-1), which in turn prevents the p53-dependent transcriptional activation of p21.

Finally, the FUCCI technology can be used for visual distinction between actively proliferating and quiescent cells. For instance, FUCCI-expressing NMuMG cells were utilized to explore cell cycle dynamics during the epithelial–mesenchyme transition (EMT).² Treatment with transforming growth factor β (TGF- β) induces EMT in normal murine mammary gland (NMuMG) cells,⁷² and FUCCI markers showed that during this transition the fraction of red mKO2-hCdt1_{30–120}-expressing G1/G0 cells increased and the fraction of green mAG-hGem_{1–110}-expressing S/G2/M cells decreased.

FUCCI IN STEM CELL LINEAGES

The FUCCI technology has already proven to be an effective tool for delineating the connection between cell cycle phasing and stem cell differentiation (see also Box 1). A recent study took advantage of the fact that the length of the G1 phase in neuronal stem cells nearly doubles during differentiation to FACS-isolate neuronal stem cells from heterologous populations based on their FUCCI signatures.⁶⁷ Furthermore, they demonstrated that FUCCI-derived cell cycle parameters could be utilized to isolate rare cells that have acquired an iPS cell-like state, thereby increasing the efficiency of reprogramming. Likewise, Coronado et al. utilized the FUCCI method to fractionate mouse embryonic stem cells (mESCs) according to their cell

TABLE 2 | FUCCI-Expressing Cell Lines

Cell Line	Description	Species of Origin	References
BJ-hTert	Foreskin fibroblasts	Human	52, 53
EndoC- β H2	Pancreatic β cells	Human	54
hESC H9	Embryonic stem cells	Human	55
hESC WA09	Embryonic stem cells	Human	56
HeLa	Cervical cancer cells	Human	2, 16
HCT116	Colon cancer cells	Human	57–60
MKM45	Stomach adenocarcinoma cells	Human	61
RPE-1	Retinal pigment epithelial cells	Human	52, 53, 62
B16	Melanoma cells	Mouse	63
D2A1	Mammary cancer cells	Mouse	64
L1210	Lymphocytic leukemia cells	Mouse	65
mESC CGR8	Embryonic stem cells	Mouse	66
mESC E14	Embryonic stem cells	Mouse	67
NIH 3T3	Fibroblast cells	Mouse	28, 68
NMuMG	Normal murine mammary gland cells	Mouse	16
S2-R+	Derived from late embryos	<i>Drosophila</i>	36

cycle stage, and subsequently evaluated whether cell cycle phasing influences mESC differentiation.⁶⁶ This approach revealed that G1 cells differentiate more efficiently than cells in S or G2 phase. A more recent study analyzed this phenomenon in more detail and showed that the cell fate choice of hESCs depends on the abundance cyclin D1-3.⁵⁵ By fractionating hESCs according to their FUCCI signatures, Pauklin and Vallier demonstrated that only in early G1 phase, when CycD1-3 levels are low, Smad2/3 is allowed to enter the nucleus and promote endoderm differentiation. In contrast, in late G1 when CycD1-3 levels are high, CycD1-3/CDK4 phosphorylates Smad2/3, which prevents it from localizing to nucleus, thereby allowing neurectoderm specification. Finally the cell cycle signature of hematopoietic stem cells (HSCs) was analyzed in FUCCI#474/#610 mice.²⁴ This approach revealed that most HSCs express mKO2-hCdt1_{30–120}, which confirmed the generally accepted model that most HSCs in the bone marrow are in G1/G0 phase. Consistent with findings in other stem cell systems, the fraction of mAG-hGem_{1–110}-positive cells increased upon differentiation of HSCs. Interestingly, Yo et al. observed that the red fluorescence intensity varied among HSCs, implying that the mKO2-hCdt1_{30–120}-high cells reside longer in G1 phase than the mKO2-hCdt1_{30–120}-low cells. Interestingly, FACS isolated mKO2-hCdt1_{30–120}-high cells had superior performance in a competitive repopulation assay, indicating that mKO2-hCdt1_{30–120} can be used as an

additional marker for the purification of HSCs. In summary, these findings demonstrate that the FUCCI reporters are extremely useful to correlate cell cycle parameters with stem cell differentiation and may allow the development of more robust differentiation protocols.

FUCCI IN NON-MAMMALIAN MODELS

As it supports live imaging, the FUCCI system is particularly well suited for studying cell cycle dynamics during development, which motivated the construction of a zebrafish-specific FUCCI system (zFUCCI).²⁹ This was first attempted by introducing human FUCCI probes into fish. Transgenic zebrafish expressing mAG-hGem_{1–110} under control of the *hspa8* promoter worked as expected, labeling S/G2/M cells with green fluorescence. However, the mKO2-hCdt1_{30–120} probe was constantly expressed through all cell cycle phases, suggesting that the SCF^{Skp2}-mediated mechanism of Cdt1 degradation is not conserved in lower vertebrates. This setback prompted Atsushi Miyawaki's team to clone the zebrafish orthologs of Cdt1 and Geminin and to optimize them using the same strategy used to develop the human FUCCI probes. These experiments showed that a longer fragment of zebrafish Cdt1 (zCdt1_{1–190}) fused to mKO2 produces a probe with robust oscillation of red fluorescence in cultivated fish cells (Figure 4(c)). Closer inspection of the sequence revealed that zCdt1_{1–190} contains only a PIP box,

BOX 1

G1 PHASE LENGTH AND STEM CELL DIFFERENTIATION

The G1 phase is of particular importance for the balance between self-renewal and differentiation in stem cell lineages. The cell cycle of embryonic or neuronal stem cells is characterized by an extremely short G1 phase that lengthens during differentiation.¹⁰⁴ Remarkably, recent work suggests that lengthening of the G1 phase is a cause, rather than a consequence of differentiation. It is assumed that a short G1 phase may restrict the window during which differentiation cues can act, and thus maintain self-renewal and pluripotency/multipotency. Consistent with this hypothesis, several studies have demonstrated that experimental lengthening of G1 phase by manipulating G1-specific cyclin/Cdk complexes tips the scale toward differentiation, whereas experimental shortening of G1 phase keeps the cells in the pluripotent/multipotent stage.^{67,66,55,105}

but no Cy motif, suggesting that the S phase-specific CRL4^{Cdt2} ubiquitin ligase, but not the SCF ubiquitin ligase, mediates the degradation of mKO2-zCdt1₁₋₁₉₀. This pathway requires chromatin-bound PCNA, which binds to the conserved PIP box (QXRVTDF) located in the N-terminus of Cdt1.^{9,73} The activation of the CLR4^{Cdt2} E3 ligase can occur only at replication forks, and consequently the activity of this complex is restricted to S phase.^{9,10} The activity of the SCF^{Skp2} complex, by contrast, lasts from S through G2 phase.¹⁰ Notably, in the original human FUCCI system, the PIP box had to be eliminated to allow faithful oscillation of the hCdt1-based G1 marker,² suggesting that human Cdt1 might be an exception in the family of Cdt1 proteins. Similar to the original FUCCI system, deletion analysis yielded D-box containing fragments of zebrafish Geminin (zGem₁₋₁₀₀ or zGem₁₋₆₀) that can be used for the visualization of cells in S/G2/M (Figure 4(b)).

Three transgenic zebrafish strains were generated, which express either mKO2-zCdt1₁₋₁₉₀, mAG-zGem₁₋₁₀₀, or mAG-zGem₁₋₆₀ under control of the *Xenopus* EF1 α promoter⁷⁴ and subsequently cross-bred (Figure 4(d)). The combination of mKO2-zCdt1₁₋₁₉₀ and mAG-zGem₁₋₁₀₀ was named Cecyil (cell cycle illuminated), while mKO2-zCdt1₁₋₁₉₀ and mAG-zGem₁₋₆₀ was termed Cecyil2 (Table 1). Time-lapse imaging of primary cells derived from Cecyil fish showed robust oscillation of the zFUCCI

probes. As the activity of the CRL4^{Cdt2} complex is restricted to S phase, cells residing in G2 phase should in theory be positive for both zFUCCI probes and therefore appear yellow. However, time-lapse analysis did not reveal any double-positive cells, even at G1-S transitions where the mammalian FUCCI probes overlap. A likely explanation for this is that the oscillation of the zFUCCI probes has only been analyzed in relatively fast dividing cells with short G2 phases, which are too short to allow significant mKO2-zCdt1₁₋₁₉₀ re-accumulation. Despite of this limitation, the zFUCCI system was successfully used in subsequent experiments. These revealed that two waves of cell cycle transitions occur during notochord development, a remarkable detail that was not noticed before.²⁹

The activity of the EF1 α promoter diminishes at later developmental stages, thus restricting the use of the Cecyil lines to early development. To overcome this limitation, Mochizuki et al. replaced Azami Green in EF1 α -mAG-zGem₁₋₁₀₀ with the brighter mCherry.⁷⁵ In combination with GFP-tagged Histone A2,⁷⁶ EF1 α -mCherry-zGem₁₋₁₀₀ allows the detection of G1, S2/G2, and M phase in the developing zebrafish lens. Analysis of cell proliferation revealed that the cells in the lens epithelium proliferate in a stereotypical pattern that resembles the germinative zone of mice and chickens.⁷⁷⁻⁷⁹

Bouldin et al. recently released an improved version of the zFUCCI system that, in contrast to the original design, expresses both probes from a single transgene.^{33,34} This dual FUCCI construct is comprised of Flag-Cerulean-zGem₁₋₁₀₀ followed by a viral 2A peptide and Cherry-zCdt1₁₋₁₉₀ (Figure 4(e)). Instead of using the EF1 α promoter,⁷⁴ which is mostly limited to early embryonic development, the dual FUCCI system relies on the zebrafish ubiquitin promoter,⁸⁰ which is expressed ubiquitously at all embryonic stages as well as in adult fish. The 2A peptide is an autocatalytic cleavage site,⁵¹ and thus the multicistronic dual FUCCI polypeptide gives rise to iso-stoichiometric amounts of a cerulean-based S/G2/M sensor, and a Cherry-based sensor, which is detectable only during G1 phase. Bouldin et al. utilized the dual FUCCI lines to determine cell cycle phasing during zebrafish somitogenesis, and thereby found that posterior progenitor cells enter a prolonged G2 phase.³³ This prolonged G2 is due to downregulation of the phosphatase Cdc25, which is rate limiting for the G2/M transition.⁸¹ Ectopic expression of Cdc25 drives ectopic cell divisions and disrupts somitogenesis, indicating that the prolonged G2 phase is critical for the coordination of cell proliferation and morphogenesis.³³

Zebrafish

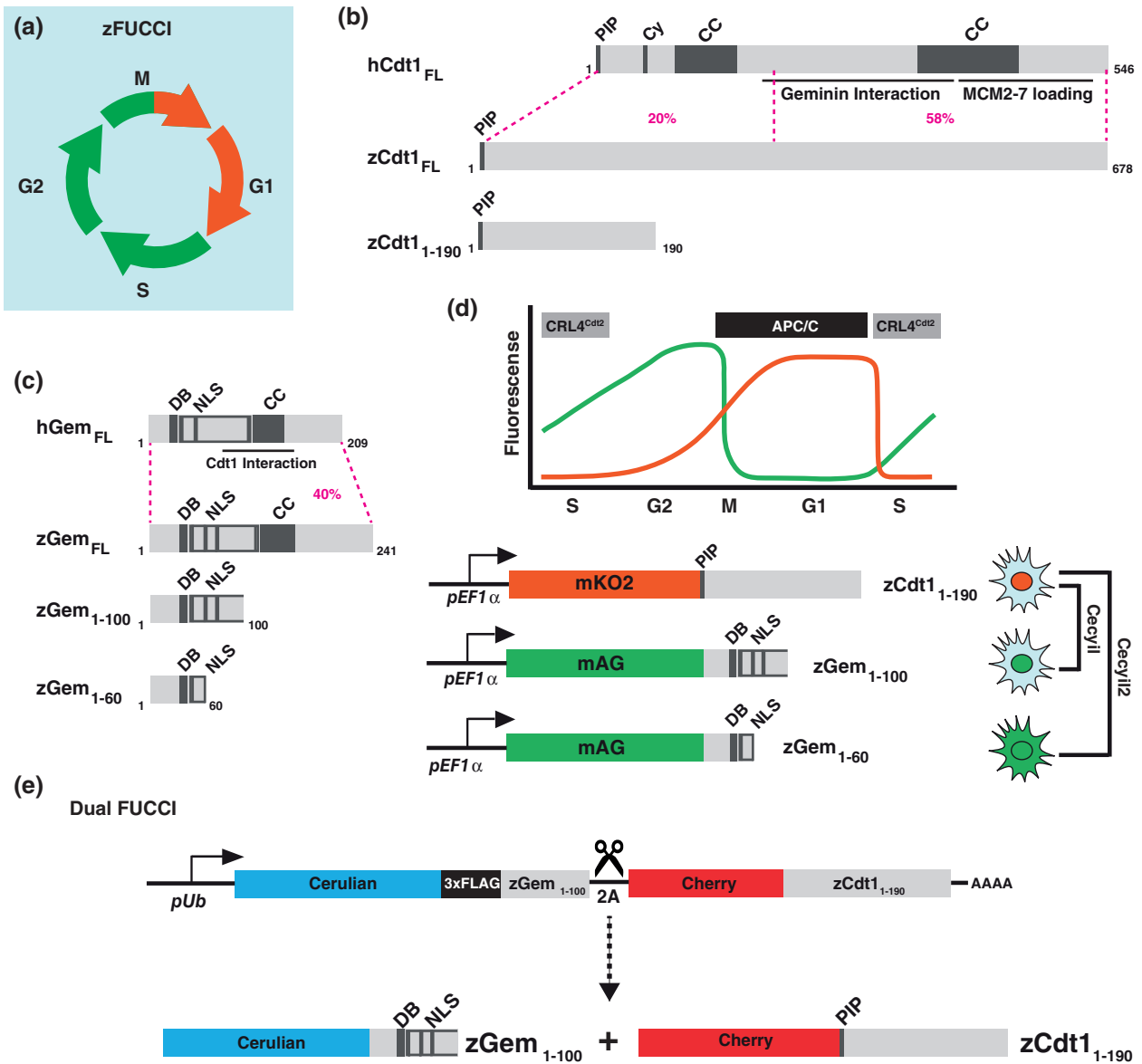


FIGURE 4 | (a) The zebrafish FUCCI systems labels cells residing in G1 phase by red fluorescence, whereas green fluorescence indicates cells in S or G2 phase. (b) Domain structure of zebrafish Cdt1 compared to human Cdt1. PIP, PCNA interaction motif; Cy, Cy motif; CC, coiled-coil domain. (c) Comparison of the functional domains of zebrafish and human Geminin. DB, destruction box; NLS, nuclear localization signal; CC, coiled-coil domain. (d) Time plot illustrating the sequential degradation of the zFUCCI probes. Nuclear mAG-zGem₁₋₁₀₀ or pan-localized mAG-zGem₁₋₆₀ accumulates during S and G2 phase, but is targeted for proteolysis during late mitotic stages and G1 phase by APC/C. The nuclear mKO-hCdt₁₋₁₉₀ probe is rapidly destroyed upon initiation of DNA replication by the S-phase-specific E3 ligase CRL4^{Cdt2}. (e) Schematic of the multicistronic dual FUCCI construct. Cerulian-3x-FLAG-zGem₁₋₁₀₀ and Cherry-zCdt₁₋₁₉₀ are expressed as a single polypeptide under the control of the zebrafish ubiquitin promoter. Both FUCCI probes are separated by a 2A sequence, which self-cleaves upon expression.

The FUCCI technology was also introduced into the urochordate *Ciona intestinalis* (sea squirt) to follow cell cycle progression in the developing embryo by real-time microscopy.⁸² For this purpose, red/green-fluorescent FUCCI probes, based on hGem₁₋₁₁₀ as well as a PIP box-containing fragment of human Cdt1 (hCdt1₁₋₁₀₀), were expressed during

embryogenesis using a ubiquitously active promoter. This approach revealed that proper formation of the neural tube also requires a prolonged G2 phase that is introduced by transcriptional downregulation of Cdc25. Misexpression of Cdc25 overrode the cell cycle delay and thereby impaired neural tube closure, further supporting the notion that cell division

and morphogenetic movements are two mutually exclusive processes that cannot occur simultaneously. Altogether, this body of work demonstrates that the FUCCI technology is a valuable tool for the visualization of developmentally programmed cell cycle changes, and hence enables us to uncover differences and similarities in the mechanisms regulating cell proliferation and morphogenesis between organs and species (see also Box 2).

The zebrafish model is not only an attractive system for the analysis of developmental processes, but it is also becoming increasingly important for whole organism screening. Thus, it is not surprising that the zFUCCI technology has been successfully utilized as a readout during chemical screens. For instance, a recent study expressed the zFUCCI probes (mCherry-zCdt1₁₋₁₉₀ and Venus-zGem₁₋₁₀₀) under control of the heart-specific *clmc2* promoter,⁸³ and used this to identify compounds that stimulate cardiomyocyte proliferation in regenerating hearts.³⁰ Another recent study used the zebrafish insulin promoter to direct the expression of the zFUCCI probes

(mKO2-zCdt1₁₋₁₉₀ and mAG-zGem₁₋₁₀₀) to pancreatic β cells,³¹ and subsequently screened for enhancers of β -cell regeneration.³²

FUCCI IN DROSOPHILA

Because of its powerful genetic toolkit and easy maintenance, the vinegar fly *Drosophila melanogaster* is one of the most versatile research model organisms. The first attempt to introduce the FUCCI method into flies relied on the original FUCCI probes that contained degrons from human Geminin and Cdt1.² However, as in zebrafish, only mAG-hGem₁₋₁₁₀, and not mKO2-hCdt1₃₀₋₁₂₀, oscillated in proliferating *Drosophila* cells. As it faithfully marks *Drosophila* cells in S, G2, and Mitosis, oscillation of mAG-hGem₁₋₁₁₀ can be used as an indicator for ongoing cell proliferation, but due the lack of a second marker it is nearly impossible to derive reliable information about the duration of individual cell cycles.^{35,84} To overcome this limitation, we recently constructed a fly-specific FUCCI system (Fly-FUCCI) that allows continuous tracking of cell cycle dynamics.³⁶ Instead of a Geminin-based probe, the Fly-FUCCI system uses an N-terminal fragment of cyclin B (dCycB₁₋₂₆₆) fused either to mRFP1 or Venus, which labels cells in S, G2, and M phases (Figure 5(b)). This fragment contains a D-box that confers APC/C-dependent proteolysis, but lacks the Cyclin box required for Cdk activation, and thus does not affect cell cycle progression. The Cdt1-based sensor used in vertebrates has been replaced by an N-terminal fragment of *Drosophila* E2F1 (dE2F1₁₋₂₀₃) fused to GFP or CFP (Figure 5(c)). This fragment contains a PIP box degron that mediates S phase-specific degradation by the CRL4^{Cdt2} ubiquitin E3 ligase, but it is unable to bind DNA or active gene transcription. Flow cytometry and live imaging demonstrated that the combined expression of both Fly-FUCCI probes allows the distinction of G1, S, and G2 phases, thus enabling accurate tracking of cell cycle transitions.³⁶ Cells in G1 phase exhibited high levels of GFP-dE2F1₁₋₂₀₃, but were devoid of mRFP1-dCycB₁₋₂₆₆. Cells in S phase, in contrast, showed low levels of GFP-dE2F1₁₋₂₀₃ and high levels of mRFP1-dCycB₁₋₂₆₆. Cells in G2 phase expressed both probes and therefore appeared yellow (Figure 5(a)). In contrast to the Geminin-based probes, dCycB₁₋₂₆₆ localizes predominantly to the cytoplasm, which improves the recognition of cell morphologies. However, the dE2F1₁₋₂₃₀-based probes are exclusively found in the nucleus. Because this differential localization of the two probes hampers automated analysis of imaging data, we also introduced the

BOX 2

THE IMPORTANCE OF G2 PHASE REGULATION DURING DEVELOPMENT

Research with tissue culture cells has focused primarily on the regulation of G1 phase and G1/S transitions, but it is becoming increasingly clear that controlling the length of G2 phase and G2/M transitions is crucial for the coordination of cell proliferation with morphogenesis during development.¹⁰⁶ The embryonic development of many species such as *Xenopus laevis* or *D. melanogaster* involves cleavage stage cycles, which are very rapid because they lack Gap phases. After a certain number of divisions, the cell cycle slows down because the maternal stockpiles of cyclins and other cell cycle regulators have been exhausted. The lengthening of the cell cycle coincides with the midblastula transition (MBT), during which the embryo initiates gene transcription.¹⁰⁷⁻¹⁰⁹ The switch to zygotic gene expression causes remodeling of the cell cycle and acquisition of a G2 phase. The phosphatase Cdc25 is rate limiting for the progression from G2 phase to mitosis in *Drosophila* and *Xenopus*.^{81,110} Deregulation of Cdc25 by mutation of its upstream regulator *tribbles* causes precocious mitotic divisions, interfering with morphogenetic movements during *Drosophila* gastrulation.¹¹¹⁻¹¹³

nuclear localization signal (NLS) of SV40 large T antigen into dCycB₁₋₂₆₆.⁸⁵ Fluorescence imaging and flow cytometry demonstrated that NLS-dCycB₁₋₂₆₆ is efficiently targeted to the nucleus and that nuclear targeting did not impair the functionality of the probe. Ubiquitously expressed FUCCI probes have only limited use for the analysis of proliferating cells in complex tissues such as the nervous system or stem cell-based epithelia. Therefore, we generated a set transgenic flies expressing the Fly-FUCCI sensors either under the UAS_t promoter⁸⁶ or the weaker germline-adapted UAS_p promoter,⁸⁷ or the QUAS promoter of the Q-system.⁸⁸ The expression of these FUCCI reporters can be activated in specific cell populations by targeted expression of their respective transcriptional activators, Gal4 and Q-factor (QF) (Figure 5(e)). Large collections of Gal4 'driver' lines have been generated, which cover virtually every *Drosophila* cell type and hence the Fly-FUCCI system can be used in a variety of experimental setups. Furthermore, the modular design facilitates the use of the Fly-FUCCI system in combination with advanced genetic tools such as MARCM⁸⁹ or the TARGET system.⁹⁰

As a proof of principle, we expressed the Fly-FUCCI system in different cell types of the adult intestinal epithelium (midgut), which is maintained by intestinal stem cells (ISCs) that differentiate into two major types of progenitor cells, enterocytes (EC), and enteroendocrine (EE) cells.⁹¹ ISC-specific expression of the Fly-FUCCI probes indicated that, under normal conditions, ISCs are arrested in either G1 or G2 phase.³⁶ However, upon enteric infection, the Fly-FUCCI system indicated increased numbers of S and G2 cells, demonstrating that changes in Fly-FUCCI signatures can be used for the detection of actively proliferating ISCs. Although a flow cytometric analysis indicated a G1 DNA content, the EE cells exhibited high levels of both GFP-dE2F1₁₋₂₃₀ and RFP-dCycB₁₋₂₆₆, implying that both APC/C and CRL4^{Cdt2} are inactive in quiescent EEs.³⁶ This is a remarkable finding, as it is generally believed that high APC/C activity is a characteristic feature of terminally differentiated cells.

Because of the low maintenance costs and their amenability to RNAi, cultured insect cells are becoming increasingly important for cell biology, biochemical experiments, and high-content screening. This prompted us to generate an optimized expression Fly-FUCCI vector for *Drosophila* cell lines (Figure 5(f)).³⁶ This multicistronic vector expresses both Fly-FUCCI probes and the neomycin resistance gene as a single polypeptide. The coding regions of these three components are separated by T2A

sequences, which auto-cleave in *Drosophila* cells.⁹² This design ensures that the two Fly-FUCCI probes are produced stoichiometrically and facilitates the selection of stable cell lines, as only cells expressing the constructs at high levels are allowed to survive.

FUCCI IN PLANTS

Because immunohistological detection is hampered by plant cell walls, genetically encoded cell cycle sensors could greatly advance the analysis cell proliferation in *Arabidopsis thaliana* and other plant species. However, the regulatory network that governs the plant cell cycle is very different from that of animals, and this complicates the transfer of the FUCCI methodology to plants. The most promising attempt to create a FUCCI-like system in plants is the recently invented CYTRAP system.⁹³ This cell cycle sensor is based on a C-terminal fragment of *Arabidopsis* Cdt1 (aCdt1₃₆₃₋₅₇₁), which is degraded at the end of G2 phase and has no impact on cell cycle progression. To restrict its expression to S and G2 phase, the sensor (aCdt1₃₆₃₋₅₇₁-RFP) was combined with the promoter of the histone H3.1-type gene HISTONE THREE RELATED2 (HRT2). The combined expression of HRT2::aCdt1₃₆₃₋₅₇₁-RFP and the G2/M-specific sensor CycB1::aCycB1-GFP⁹⁴ labels *Arabidopsis* cells from S through early G2 phase with red fluorescence and cells from late G2 to M phase with green fluorescence. Major drawbacks of the CYTRAP system are its inability to label G1 cells and to distinguish between S and G2 phase. In the future, these limitations will likely be overcome by tagging additional plant cell cycle proteins that have alternate expression profiles.

FUCCI IN NON-CANONICAL AND ABERRANT CELL CYCLES

Endoreplication cycles or endocycles are a cell cycle variant that consists only of G and S phases and thereby lead to the formation of polyploid cells.^{95,96} The increased DNA content allows a higher transcription capacity that can facilitate cellular growth, hence endocycles are often employed in cellular lineages that give rise to cells with increased metabolic output or secretory functions. A regulative network that includes phase-shifted oscillations of APC/C and CRL4^{Cdt2} activities, analogous to those seen in mitotic cells, mediates the endocycles in *Drosophila* salivary glands.^{95,96} The endocycles in the *Drosophila* salivary gland occur asynchronously and as a consequence result in expression of the Fly-FUCCI probes in cells that are labeled by either green *ub*-GFP^{-E2F11-230}

Flies

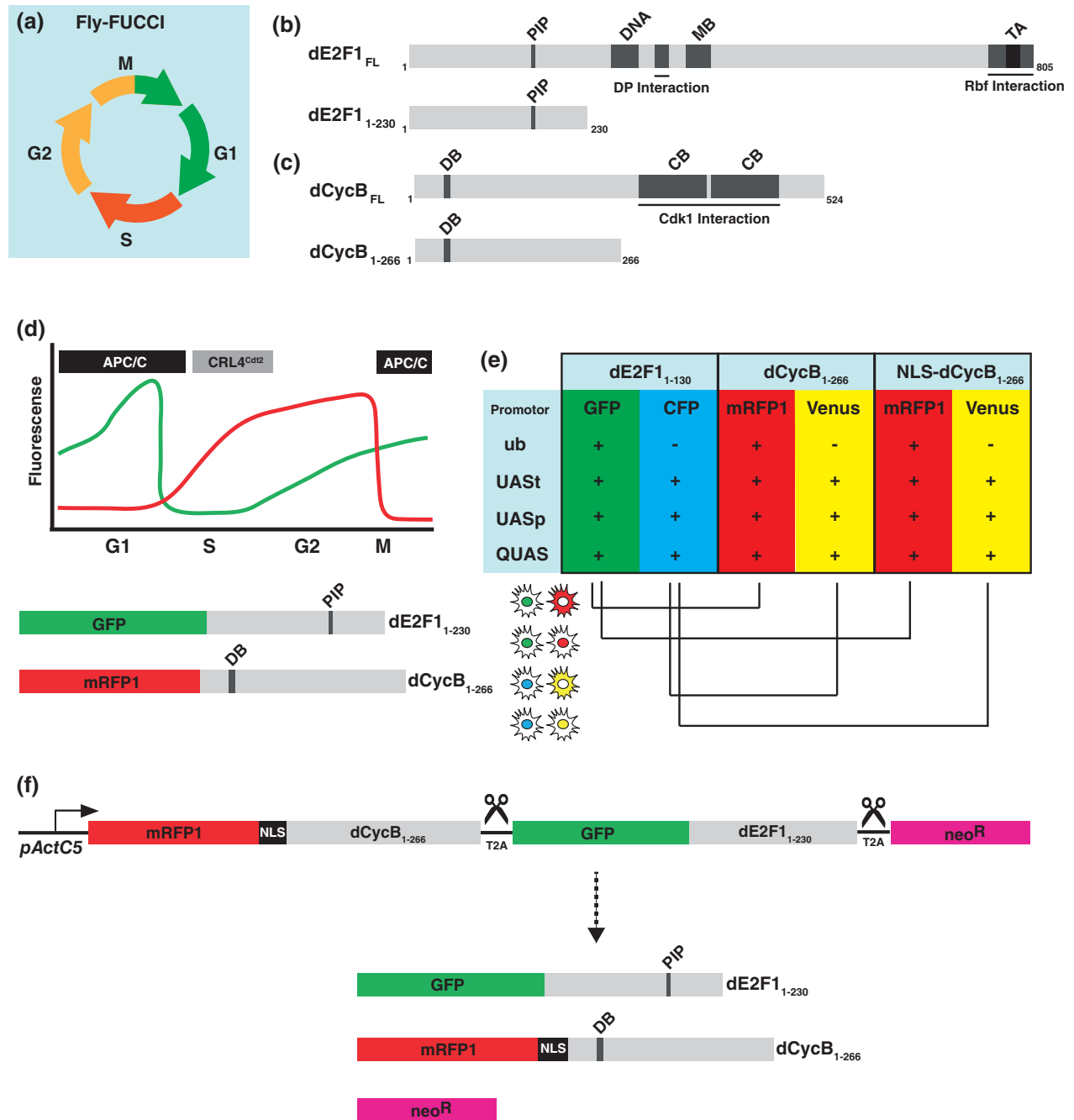


FIGURE 5 | FUCCI in flies. (a) Fly-FUCCI marks cells in G1 phase in green, cells in S phase are labeled in red, and cells in G2 phase express both markers and therefore appear yellow. (b) Domain structure of *Drosophila* E2F1. PIP, PCNA interaction motif; DNA, DNA binding motif; MB, marked box; TA, transactivation domain. (c) Schematic of *Drosophila* cyclin B. DB, destruction box; CB, cyclin box. (d) Time plot illustrating the sequential destruction of the Fly-FUCCI probes. GFP-E2F1₁₋₂₃₀ accumulates during G1 phase, but is rapidly destroyed during S phase by CRL4^{Cdt2}-mediated degradation. Levels of GFP-E2F1₁₋₂₃₀ recover during G2 phase. mRFP1-CycB₁₋₂₆₆ degradation is mediated by APC/C and lasts from mid-mitosis throughout G1 phase. Levels of mRFP1-CycB₁₋₂₆₆ increase in S phase and reach their maximum at the end of G2 phase. (e) Table describing the promoter/fluorochrome combinations of the currently available Fly-FUCCI transgenes. (f) Schematic of the multicistronic Fly-FUCCI construct that has been optimized for the use in *Drosophila* cell lines. T2A autocleavage sites separate both, the Fly-FUCCI probes and the neomycin resistance gene, thereby allowing rapid selection of stable cell lines.

(G phase) or red ub-mRFP1-CycB₁₋₂₆₆ (S phase).³⁶ A striking example for the importance of endocycles for tissue regeneration is found in the EC of the adult *Drosophila* midgut. These cells execute several endocycles as part of their normal differentiation program and thereby attain DNA contents between 8C and 32C. EC-specific expression of the Fly-FUCCI probes revealed that terminally arrested ECs arrest with low CRL4^{Cdt2} and high APC/C activity,³⁶ similar to many G0-arrested mammalian cells. However, the level of the APC/C-sensitive mRFP1-CycB₁₋₂₆₆ probe dramatically increased upon enteric infection with *Pseudomonas entomophila*, reflecting the periodic suppression of APC/C activity that occurs during endocycle S phases.^{95,96} Consistently, endocycling ECs also exhibited periodic loss of the CRL4^{Cdt2}-sensitive GFP-E2F1₁₋₂₃₀ probe during S phases, demonstrating that the Fly-FUCCI system can faithfully distinguish endocycling from arrested ECs.

Similarly, FUCCI#596/#504 mice were utilized to visualize endocycle oscillations in the trophoblast cell lineage.²² As in *Drosophila*, endocycling in the trophoblast cell lineage involves many of the cell cycle regulators found in mitotic cells including APC/C and SCF^{Skp2}.^{95,96} Live imaging of FUCCI-expressing trophoblast giant cells revealed that both E3 ligases are sequentially activated during endocycling. However, endocycles are not the only road to polyploidy, and endomitosis is another non-canonical cell cycle variant that leads to the formation of polyploid cells.⁹⁵ Endomitotic cells such as megakaryocytes execute an abortive mitotic cell cycle that lacks an anaphase B as well as cytokinesis. The FUCCI#610/#474 mice showed good expression in the bone marrow and thus were used to visualize the cell cycle oscillations of megakaryocytes.²² This analysis revealed that cells with lower polyploidy (<16C) cycle faster than cells with high polyploidy (>16C).

The FUCCI technology has also proven to be valuable as a tool for the detection of aberrant cell cycles. For instance, real-time imaging revealed that treatment of FUCCI-expressing NMuMG cells with the topoisomerase II inhibitor, Etoposide, results in a transient G2 arrest followed by mitosis-independent oscillation of the FUCCI probes. Likewise, live imaging of FUCCI-expressing MEFs demonstrated that persistent telomere dysfunction causes a prolonged G2 phase followed by endocycles.⁹⁷ Because endocycling is a common mechanism for the formation of polyploid cells,^{95,96} it was suggested that telomere dysfunction might represent a novel mechanism for the formation of aneuploid cancer cells. Another interesting application comes from a recent study aimed at elucidating the mechanism of

p53 activation in drug-induced tetraploid cells.⁶² To address this question, the team of David Pellman had to overcome the problem that tetraploid G1 cells have the same DNA content as diploid G2 cells, which makes it nearly impossible to separate both populations by standard DNA detection-based flow cytometry. The solution was to combine FACS-sorting with FUCCI markers. The fact that diploid G2 cells express mKO2-hGem₁₋₁₁₀, whereas tetraploid G1 cells express mAG-hCdt1₃₀₋₁₂₀, allowed Pellman's group to FACS sort true tetraploid cells, which were then utilized for RNAi screening. In summary, these studies underscore the value of the FUCCI method for analyzing irregular cell cycles and may help us to eventually understand the connection between polyploidy and tumor formation.

PERSPECTIVE

In summary, the Fly-FUCCI technology represents a widely applicable method for the analysis of cell cycle oscillations in living cells. The FUCCI method has been introduced in all major model systems except *C. elegans* to study a broad range of topics such as stem cell differentiation, the coordination of proliferation with morphogenic processes, tissue regeneration, T cell activation, system level analysis of cell cycle oscillations, and drug screening. Furthermore, we anticipate that the combination FUCCI sensors and flow cytometry will have widespread applications in the future.

A disadvantage that all FUCCI sensors have in common is that they cannot precisely detect the transition from S to G2 phase. A simple solution for this problem could be to integrate an S phase marker such as PCNA-GFP⁹⁸ into the FUCCI system. Another drawback of the current generation FUCCI sensors is that they cannot discriminate between G0 and G1 phases. A recent study reported that a Venus-tagged p27 mutant lacking the CDK inhibitory activity (mVenus-p27K-) can be used in combination with FUCCI probes to discriminate between cells in G0 and G1 phases during cell cycle re-entry after serum stimulation.⁹⁹ However, this combination of markers failed to detect G0 cells during early stages of cell cycle exit upon serum withdrawal, and the corresponding mice strains suffered from low expression levels in certain tissues. If these problems can be overcome in the future, this approach could be a significant improvement to the FUCCI technology. The recent work on mice and flies indicated that lineage-restricted expression of the FUCCI sensors greatly enhances their utility for analyzing the coordination of cell

proliferation and differentiation. Therefore, we believe that the FUCCI sensors for other model organisms (e.g., Zebrafish and *Arabidopsis*) should also be modified so that their expression can be controlled in space and time. The most promising approach to achieve this goal appears to be the use of binary expression such as the Gal4/UAS system. In zebrafish, the Gal4/UAS system was introduced some

time ago,¹⁰⁰ but only recently has the Gal4 activator been combined with the Tol2 transposable element,¹⁰¹ which enabled the generation of a large collection of fish lines that express Gal4 in specific cells, tissues, and organs.¹⁰² The Gal4/UAS method has recently been established in *Arabidopsis*.¹⁰³ These advances pave the way for the development of conditional versions of zFUCCI and CYTRAP, respectively.

ACKNOWLEDGMENTS

We thank Cortney Bouldin and David Kimelman for helpful discussions about the zebrafish FUCCI system. Furthermore, we apologize to the authors whose work could not be mentioned due to space restrictions. The work on the Fly-FUCCI technology was funded by the DKFZ, ERC Advanced Grant 268515, and DFG SFB 873.

REFERENCES

1. Nasmyth K. A prize for proliferation. *Cell* 2001, 107:689–701.
2. Sakaue-Sawano A, Kurokawa H, Morimura T, Hanyu A, Hama H, Osawa H, Kashiwagi S, Fukami K, Miyata T, Miyoshi H, et al. Visualizing spatiotemporal dynamics of multicellular cell-cycle progression. *Cell* 2008, 132:487–498.
3. Arias EE, Walter JC. Strength in numbers: preventing rereplication via multiple mechanisms in eukaryotic cells. *Genes Dev* 2007, 21:497–518.
4. Nishitani H, Lygerou Z, Nishimoto T. Proteolysis of DNA replication licensing factor Cdt1 in S-phase is performed independently of geminin through its N-terminal region. *J Biol Chem* 2004, 279:30807–30816.
5. Li X, Zhao Q, Liao R, Sun P, Wu X. The SCF(Skp2) ubiquitin ligase complex interacts with the human replication licensing factor Cdt1 and regulates Cdt1 degradation. *J Biol Chem* 2003, 278:30854–30858.
6. McGarry TJ, Kirschner MW. Geminin, an inhibitor of DNA replication, is degraded during mitosis. *Cell* 1998, 93:1043–1053.
7. Wei W, Ayad NG, Wan Y, Zhang GJ, Kirschner MW, Kaelin WG Jr. Degradation of the SCF component Skp2 in cell-cycle phase G1 by the anaphase-promoting complex. *Nature* 2004, 428:194–198.
8. Bashir T, Dorrello NV, Amador V, Guardavaccaro D, Pagano M. Control of the SCF(Skp2-Cks1) ubiquitin ligase by the APC/C(Cdh1) ubiquitin ligase. *Nature* 2004, 428:190–193.
9. Arias EE, Walter JC. PCNA functions as a molecular platform to trigger Cdt1 destruction and prevent re-replication. *Nat Cell Biol* 2006, 8:84–90.
10. Nishitani H, Sugimoto N, Roukos V, Nakanishi Y, Saijo M, Obuse C, Tsurimoto T, Nakayama KI, Nakayama K, Fujita M, et al. Two E3 ubiquitin ligases, SCF-Skp2 and DDB1-Cul4, target human Cdt1 for proteolysis. *EMBO J* 2006, 25:1126–1136.
11. Cook JG, Chasse DA, Nevins JR. The regulated association of Cdt1 with minichromosome maintenance proteins and Cdc6 in mammalian cells. *J Biol Chem* 2004, 279:9625–9633.
12. Ferenbach A, Li A, Brito-Martins M, Blow JJ. Functional domains of the *Xenopus* replication licensing factor Cdt1. *Nucleic Acids Res* 2005, 33:316–324.
13. Yanagi K, Mizuno T, You Z, Hanaoka F. Mouse geminin inhibits not only Cdt1-MCM6 interactions but also a novel intrinsic Cdt1 DNA binding activity. *J Biol Chem* 2002, 277:40871–40880.
14. Hall JR, Lee HO, Bunker BD, Dorn ES, Rogers GC, Duronio RJ, Cook JG. Cdt1 and Cdc6 are destabilized by rereplication-induced DNA damage. *J Biol Chem* 2008, 283:25356–25363.
15. Lee C, Hong B, Choi JM, Kim Y, Watanabe S, Ishimi Y, Enomoto T, Tada S, Cho Y. Structural basis for inhibition of the replication licensing factor Cdt1 by geminin. *Nature* 2004, 430:913–917.
16. Sakaue-Sawano A, Kobayashi T, Ohtawa K, Miyawaki A. Drug-induced cell cycle modulation leading to cell-cycle arrest, nuclear mis-segregation, or endoreplication. *BMC Cell Biol* 2011, 12:2.
17. Benjamin JM, Torke SJ, Demeler B, McGarry TJ. Geminin has dimerization, Cdt1-binding, and destruction domains that are required for biological activity. *J Biol Chem* 2004, 279:45957–45968.
18. Okorokov AL, Orlova EV, Kingsbury SR, Bagneris C, Gohlke U, Williams GH, Stoeber K. Molecular structure of human geminin. *Nat Struct Mol Biol* 2004, 11:1021–1022.

19. Saxena S, Yuan P, Dhar SK, Senga T, Takeda D, Robinson H, Kornbluth S, Swaminathan K, Dutta A. A dimerized coiled-coil domain and an adjoining part of geminin interact with two sites on Cdt1 for replication inhibition. *Mol Cell* 2004, 15:245–258.
20. Boos A, Lee A, Thompson DM, Kroll KL. Subcellular translocation signals regulate Geminin activity during embryonic development. *Biol Cell* 2006, 98:363–375.
21. Sakaue-Sawano A, Ohtawa K, Hama H, Kawano M, Ogawa M, Miyawaki A. Tracing the silhouette of individual cells in S/G2/M phases with fluorescence. *Chem Biol* 2008, 15:1243–1248.
22. Sakaue-Sawano A, Hoshida T, Yo M, Takahashi R, Ohtawa K, Arai T, Takahashi E, Noda S, Miyoshi H, Miyawaki A. Visualizing developmentally programmed endoreplication in mammals using ubiquitin oscillators. *Development* 2013, 140:4624–4632.
23. Ge WP, Miyawaki A, Gage FH, Jan YN, Jan LY. Local generation of glia is a major astrocyte source in postnatal cortex. *Nature* 2012, 484:376–380.
24. Yo M, Sakaue-Sawano A, Noda S, Miyawaki A, Miyoshi H. Fucci-guided purification of hematopoietic stem cells with high repopulating activity. *Biochem Biophys Res Commun* 2015, 457:7–11.
25. Aiba Y, Kometani K, Hamadate M, Moriyama S, Sakaue-Sawano A, Tomura M, Luche H, Fehling HJ, Casellas R, Kanagawa O, et al. Preferential localization of IgG memory B cells adjacent to contracted germinal centers. *Proc Natl Acad Sci USA* 2010, 107:12192–12197.
26. Abe T, Sakaue-Sawano A, Kiyonari H, Shioi G, Inoue K, Horiuchi T, Nakao K, Miyawaki A, Aizawa S, Fujimori T. Visualization of cell cycle in mouse embryos with Fucci2 reporter directed by Rosa26 promoter. *Development* 2013, 140:237–246.
27. Juuri E, Saito K, Ahtiainen L, Seidel K, Tummers M, Hochedlinger K, Klein OD, Thesleff I, Michon F. Sox2+ stem cells contribute to all epithelial lineages of the tooth via Sfrp5+ progenitors. *Dev Cell* 2012, 23:317–328.
28. Mort RL, Ford MJ, Sakaue-Sawano A, Lindstrom NO, Casadio A, Douglas AT, Keighren MA, Hohenstein P, Miyawaki A, Jackson IJ. Fucci2a: a bicistronic cell cycle reporter that allows Cre mediated tissue specific expression in mice. *Cell Cycle* 2014, 13:2681–2696.
29. Sugiyama M, Sakaue-Sawano A, Iimura T, Fukami K, Kitaguchi T, Kawakami K, Okamoto H, Higashijima S, Miyawaki A. Illuminating cell-cycle progression in the developing zebrafish embryo. *Proc Natl Acad Sci USA* 2009, 106:20812–20817.
30. Choi WY, Gemberling M, Wang J, Holdway JE, Shen MC, Karlstrom RO, Poss KD. In vivo monitoring of cardiomyocyte proliferation to identify chemical modifiers of heart regeneration. *Development* 2013, 140:660–666.
31. Ninov N, Hesselson D, Gut P, Zhou A, Fidelin K, Stainier DY. Metabolic regulation of cellular plasticity in the pancreas. *Curr Biol* 2013, 23:1242–1250.
32. Tsuji N, Ninov N, Delawary M, Osman S, Roh AS, Gut P, Stainier DY. Whole organism high content screening identifies stimulators of pancreatic β -cell proliferation. *PLoS One* 2014, 9:e104112.
33. Bouldin CM, Snelson CD, Farr GH 3rd, Kimelman D. Restricted expression of cdc25a in the tailbud is essential for formation of the zebrafish posterior body. *Genes Dev* 2014, 28:384–395.
34. Bouldin CM, Kimelman D. Dual fucci: a new transgenic line for studying the cell cycle from embryos to adults. *Zebrafish* 2014, 11:182–183.
35. Nakajima Y, Kuranaga E, Sugimura K, Miyawaki A, Miura M. Nonautonomous apoptosis is triggered by local cell cycle progression during epithelial replacement in *Drosophila*. *Mol Cell Biol* 2011, 31:2499–2512.
36. Zielke N, Korzelius J, van Straaten M, Bender K, Schuhknecht GF, Dutta D, Xiang J, Edgar BA. Fly-FUCCI: a versatile tool for studying cell proliferation in complex tissues. *Cell Rep* 2014, 7:588–598.
37. Niwa H, Yamamura K, Miyazaki J. Efficient selection for high-expression transfectants with a novel eukaryotic vector. *Gene* 1991, 108:193–199.
38. Hashimoto H, Yuasa S, Tabata H, Tohyama S, Hayashiji N, Hattori F, Muraoka N, Egashira T, Okata S, Yae K, et al. Time-lapse imaging of cell cycle dynamics during development in living cardiomyocyte. *J Mol Cell Cardiol* 2014, 72:241–249.
39. Griswold SL, Sajja KC, Jang CW, Behringer RR. Generation and characterization of iUBC-KikGR photoconvertible transgenic mice for live time-lapse imaging during development. *Genesis* 2011, 49:591–598.
40. Rhee JM, Purity MK, Lackan CS, Long JZ, Kondoh G, Takeda J, Hadjantonakis AK. In vivo imaging and differential localization of lipid-modified GFP-variant fusions in embryonic stem cells and mice. *Genesis* 2006, 44:202–218.
41. Kisseberth WC, Brettingen NT, Lohse JK, Sandgren EP. Ubiquitous expression of marker transgenes in mice and rats. *Dev Biol* 1999, 214:128–138.
42. Potts W, Tucker D, Wood H, Martin C. Chicken β -globin 5'HS4 insulators function to reduce variability in transgenic founder mice. *Biochem Biophys Res Commun* 2000, 273:1015–1018.
43. Stewart MD, Jang CW, Hong NW, Austin AP, Behringer RR. Dual fluorescent protein reporters for studying cell behaviors in vivo. *Genesis* 2009, 47:708–717.
44. Friedrich G, Soriano P. Promoter traps in embryonic stem cells: a genetic screen to identify and mutate developmental genes in mice. *Genes Dev* 1991, 5:1513–1523.

45. Soriano P. Generalized lacZ expression with the ROSA26 Cre reporter strain. *Nat Genet* 1999, 21: 70–71.
46. Zambrowicz BP, Imamoto A, Fiering S, Herzenberg LA, Kerr WG, Soriano P. Disruption of overlapping transcripts in the ROSA β geo 26 gene trap strain leads to widespread expression of β -galactosidase in mouse embryos and hematopoietic cells. *Proc Natl Acad Sci USA* 1997, 94:3789–3794.
47. Srinivas S, Watanabe T, Lin CS, Williams CM, Tanabe Y, Jessell TM, Costantini F. Cre reporter strains produced by targeted insertion of EYFP and ECFP into the ROSA26 locus. *BMC Dev Biol* 2001, 1:4.
48. Shioi G, Kiyonari H, Abe T, Nakao K, Fujimori T, Jang CW, Huang CC, Akiyama H, Behringer RR, Aizawa S. A mouse reporter line to conditionally mark nuclei and cell membranes for in vivo live-imaging. *Genesis* 2011, 49:570–578.
49. Lakso M, Pichel JG, Gorman JR, Sauer B, Okamoto Y, Lee E, Alt FW, Westphal H. Efficient in vivo manipulation of mouse genomic sequences at the zygote stage. *Proc Natl Acad Sci USA* 1996, 93:5860–5865.
50. Abe T, Kiyonari H, Shioi G, Inoue K, Nakao K, Aizawa S, Fujimori T. Establishment of conditional reporter mouse lines at ROSA26 locus for live cell imaging. *Genesis* 2011, 49:579–590.
51. de Felipe P, Luke GA, Hughes LE, Gani D, Halpin C, Ryan MD. E unum pluribus: multiple proteins from a self-processing polyprotein. *Trends Biotechnol* 2006, 24:68–75.
52. Krenning L, Feringa FM, Shaltiel IA, van den Berg J, Medema RH. Transient activation of p53 in G2 phase is sufficient to induce senescence. *Mol Cell* 2014, 55:59–72.
53. Shaltiel IA, Aprelia M, Saurin AT, Chowdhury D, Kops GJ, Voest EE, Medema RH. Distinct phosphatases antagonize the p53 response in different phases of the cell cycle. *Proc Natl Acad Sci USA* 2014, 111:7313–7318.
54. Carlier G, Maugein A, Cordier C, Pechberty S, Garfa-Traore M, Martin P, Scharfmann R, Albagli O. Human fucci pancreatic β cell lines: new tools to study β cell cycle and terminal differentiation. *PLoS One* 2014, 9:e108202.
55. Pauklin S, Vallier L. The cell-cycle state of stem cells determines cell fate propensity. *Cell* 2013, 155:135–147.
56. Singh AM, Chappell J, Trost R, Lin L, Wang T, Tang J, Matlock BK, Weller KP, Wu H, Zhao S, et al. Cell-cycle control of developmentally regulated transcription factors accounts for heterogeneity in human pluripotent cells. *Stem Cell Rep* 2013, 1:532–544.
57. Kleiblova P, Shaltiel IA, Benada J, Sevcik J, Pechackova S, Pohlreich P, Voest EE, Dundr P, Bartek J, Kleibl Z, et al. Gain-of-function mutations of PPM1D/Wip1 impair the p53-dependent G1 checkpoint. *J Cell Biol* 2013, 201:511–521.
58. Bao Y, Mukai K, Hishiki T, Kubo A, Ohmura M, Sugiura Y, Matsuura T, Nagahata Y, Hayakawa N, Yamamoto T, et al. Energy management by enhanced glycolysis in G1-phase in human colon cancer cells in vitro and in vivo. *Mol Cancer Res* 2013, 11:973–985.
59. Kagawa Y, Matsumoto S, Kamioka Y, Mimori K, Naito Y, Ishii T, Okuzaki D, Nishida N, Maeda S, Naito A, et al. Cell cycle-dependent Rho GTPase activity dynamically regulates cancer cell motility and invasion in vivo. *PLoS One* 2013, 8:e83629.
60. Sionov RV, Netzer E, Shaulian E. Differential regulation of FBXW7 isoforms by various stress stimuli. *Cell Cycle* 2013, 12:3547–3554.
61. Yano S, Miwa S, Mii S, Hiroshima Y, Uehara F, Yamamoto M, Kishimoto H, Tazawa H, Bouvet M, Fujiwara T, et al. Invading cancer cells are predominantly in G0/G1 resulting in chemoresistance demonstrated by real-time FUCCI imaging. *Cell Cycle* 2014, 13:953–960.
62. Ganem NJ, Cornils H, Chiu SY, O'Rourke KP, Arnaud J, Yimlamai D, Thery M, Camargo FD, Pellman D. Cytokinesis failure triggers hippo tumor suppressor pathway activation. *Cell* 2014, 158:833–848.
63. Matsushita H, Hosoi A, Ueha S, Abe J, Fujieda N, Tomura M, Maekawa R, Matsushima K, Ohara O, Kakimi K. Cytotoxic T lymphocytes block tumor growth both by lytic activity and IFN- γ -dependent cell cycle arrest. *Cancer Immunol Res* 2015, 3:26–36.
64. Bouchard G, Bouvette G, Therriault H, Bujold R, Saucier C, Paquette B. Pre-irradiation of mouse mammary gland stimulates cancer cell migration and development of lung metastases. *Br J Cancer* 2013, 109:1829–1838.
65. Son S, Tzur A, Weng Y, Jorgensen P, Kim J, Kirschner MW, Manalis SR. Direct observation of mammalian cell growth and size regulation. *Nat Methods* 2012, 9:910–912.
66. Coronado D, Godet M, Bourillot PY, Tapponnier Y, Bernat A, Petit M, Afanassieff M, Markossian S, Malashicheva A, Iacone R, et al. A short G1 phase is an intrinsic determinant of naive embryonic stem cell pluripotency. *Stem Cell Res* 2013, 10:118–131.
67. Roccio M, Schmitter D, Knobloch M, Okawa Y, Sage D, Lutolf MP. Predicting stem cell fate changes by differential cell cycle progression patterns. *Development* 2013, 140:459–470.
68. Feillet C, Krusche P, Tamanini F, Janssens RC, Downey MJ, Martin P, Teboul M, Saito S, Levi FA, Bretschneider T, et al. Phase locking and multiple oscillating attractors for the coupled mammalian clock and cell cycle. *Proc Natl Acad Sci USA* 2014, 111:9828–9833.
69. Slaats GG, Ghosh AK, Falke LL, Le Corre S, Shaltiel IA, van de Hoek G, Klasson TD, Stokman MF, Logister I, Verhaar MC, et al. Nephronophthisis-

- associated cep164 regulates cell cycle progression, apoptosis and epithelial-to-mesenchymal transition. *PLoS Genet* 2014, 10:e1004594.
70. Sabherwal N, Thuret R, Lea R, Stanley P, Papalopulu N. aPKC phosphorylates p27Xic1, providing a mechanistic link between apicobasal polarity and cell-cycle control. *Dev Cell* 2014, 31:559–571.
 71. Santos SD, Wollman R, Meyer T, Ferrell JE Jr. Spatial positive feedback at the onset of mitosis. *Cell* 2012, 149:1500–1513.
 72. Piek E, Moustakas A, Kurisaki A, Heldin CH, ten Dijke P. TGF- β type I receptor/ALK-5 and Smad proteins mediate epithelial to mesenchymal transdifferentiation in NMuMG breast epithelial cells. *J Cell Sci* 1999, 112(Pt 24):4557–4568.
 73. Havens CG, Walter JC. Docking of a specialized PIP Box onto chromatin-bound PCNA creates a degron for the ubiquitin ligase CRL4Cdt2. *Mol Cell* 2009, 35:93–104.
 74. Urasaki A, Morvan G, Kawakami K. Functional dissection of the Tol2 transposable element identified the minimal cis-sequence and a highly repetitive sequence in the subterminal region essential for transposition. *Genetics* 2006, 174:639–649.
 75. Mochizuki T, Suzuki S, Masai I. Spatial pattern of cell geometry and cell-division orientation in zebrafish lens epithelium. *Biol Open* 2014, 3:982–994.
 76. Pauls S, Geldmacher-Voss B, Campos-Ortega JA. A zebrafish histone variant H2A.F/Z and a transgenic H2A.F/Z:GFP fusion protein for in vivo studies of embryonic development. *Dev Genes Evol* 2001, 211:603–610.
 77. Modak SP, Morris G, Yamada T. DNA synthesis and mitotic activity during early development of chick lens. *Dev Biol* 1968, 17:544–561.
 78. Zhou M, Leiberman J, Xu J, Lavker RM. A hierarchy of proliferative cells exists in mouse lens epithelium: implications for lens maintenance. *Invest Ophthalmol Vis Sci* 2006, 47:2997–3003.
 79. McAvoy JW. Cell division, cell elongation and distribution of α -, β - and γ -crystallins in the rat lens. *J Embryol Exp Morphol* 1978, 44:149–165.
 80. Mosimann C, Kaufman CK, Li P, Pugach EK, Tamplin OJ, Zon LI. Ubiquitous transgene expression and Cre-based recombination driven by the ubiquitin promoter in zebrafish. *Development* 2011, 138:169–177.
 81. Edgar BA, Sprenger F, Duronio RJ, Leopold P, O'Farrell PH. Distinct molecular mechanisms regulate cell cycle timing at successive stages of *Drosophila* embryogenesis. *Genes Dev* 1994, 8:440–452.
 82. Ogura Y, Sakaue-Sawano A, Nakagawa M, Satoh N, Miyawaki A, Sasakura Y. Coordination of mitosis and morphogenesis: role of a prolonged G2 phase during chordate neurulation. *Development* 2011, 138:577–587.
 83. Rottbauer W, Saurin AJ, Lickert H, Shen X, Burns CG, Wo ZG, Kemler R, Kingston R, Wu C, Fishman M. Reptin and pontin antagonistically regulate heart growth in zebrafish embryos. *Cell* 2002, 111:661–672.
 84. Karpowicz P, Zhang Y, Hogenesch JB, Emery P, Perrimon N. The circadian clock gates the intestinal stem cell regenerative state. *Cell Rep* 2013, 3:996–1004.
 85. Gorlich D, Mattaj JW. Nucleocytoplasmic transport. *Science* 1996, 271:1513–1518.
 86. Brand AH, Perrimon N. Targeted gene expression as a means of altering cell fates and generating dominant phenotypes. *Development* 1993, 118:401–415.
 87. Rorth P. Gal4 in the *Drosophila* female germline. *Mech Dev* 1998, 78:113–118.
 88. Potter CJ, Tasic B, Russler EV, Liang L, Luo L. The Q system: a repressible binary system for transgene expression, lineage tracing, and mosaic analysis. *Cell* 2010, 141:536–548.
 89. Lee T, Luo L. Mosaic analysis with a repressible cell marker (MARCM) for *Drosophila* neural development. *Trends Neurosci* 2001, 24:251–254.
 90. McGuire SE, Mao Z, Davis RL. Spatiotemporal gene expression targeting with the TARGET and gene-switch systems in *Drosophila*. *Sci STKE* 2004, 2004:pl6.
 91. Jiang H, Edgar BA. Intestinal stem cell function in *Drosophila* and mice. *Curr Opin Genet Dev* 2012, 22:354–360.
 92. Gonzalez M, Martin-Ruiz I, Jimenez S, Pirone L, Barrio R, Sutherland JD. Generation of stable *Drosophila* cell lines using multicistronic vectors. *Sci Rep* 2011, 1:75.
 93. Yin K, Ueda M, Takagi H, Kajihara T, Sugamata Aki S, Nobusawa T, Umeda-Hara C, Umeda M. A dual-color marker system for in vivo visualization of cell cycle progression in *Arabidopsis*. *Plant J* 2014, 80:541–552.
 94. Ubeda-Tomas S, Federici F, Casimiro I, Beemster GT, Bhalerao R, Swarup R, Doerner P, Haseloff J, Bennett MJ. Gibberellin signaling in the endodermis controls *Arabidopsis* root meristem size. *Curr Biol* 2009, 19:1194–1199.
 95. Edgar BA, Zielke N, Gutierrez C. Endocycles: a recurrent evolutionary innovation for post-mitotic cell growth. *Nat Rev Mol Cell Biol* 2014, 15:197–210.
 96. Zielke N, Edgar BA, Depamphilis ML. Endoreplication. *Cold Spring Harb Perspect Biol* 2013, 5:a012948. doi: 10.1101/cshperspect.a012948.
 97. Davoli T, Denchi EL, de Lange T. Persistent telomere damage induces bypass of mitosis and tetraploidy. *Cell* 2010, 141:81–93.
 98. Leonhardt H, Rahn HP, Weinzierl P, Sporbert A, Cremer T, Zink D, Cardoso MC. Dynamics of DNA replication factories in living cells. *J Cell Biol* 2000, 149:271–280.

99. Oki T, Nishimura K, Kitaura J, Togami K, Maehara A, Izawa K, Sakaue-Sawano A, Niida A, Miyano S, Aburatani H, et al. A novel cell-cycle-indicator, mVenus-p27K-, identifies quiescent cells and visualizes G0-G1 transition. *Sci Rep* 2014, 4:4012.
100. Scheer N, Campos-Ortega JA. Use of the Gal4-UAS technique for targeted gene expression in the zebrafish. *Mech Dev* 1999, 80:153–158.
101. Scott EK, Mason L, Arrenberg AB, Ziv L, Gosse NJ, Xiao T, Chi NC, Asakawa K, Kawakami K, Baier H. Targeting neural circuitry in zebrafish using GAL4 enhancer trapping. *Nat Methods* 2007, 4: 323–326.
102. Asakawa K, Suster ML, Mizusawa K, Nagayoshi S, Kotani T, Urasaki A, Kishimoto Y, Hibi M, Kawakami K. Genetic dissection of neural circuits by Tol2 transposon-mediated Gal4 gene and enhancer trapping in zebrafish. *Proc Natl Acad Sci USA* 2008, 105:1255–1260.
103. Waki T, Miyashima S, Nakanishi M, Ikeda Y, Hashimoto T, Nakajima K. A GAL4-based targeted activation tagging system in *Arabidopsis thaliana*. *Plant J* 2013, 73:357–367.
104. Lange C, Calegari F. Cdks and cyclins link G1 length and differentiation of embryonic, neural and hematopoietic stem cells. *Cell Cycle* 2010, 9: 1893–1900.
105. Lange C, Huttner WB, Calegari F. Cdk4/cyclinD1 overexpression in neural stem cells shortens G1, delays neurogenesis, and promotes the generation and expansion of basal progenitors. *Cell Stem Cell* 2009, 5:320–331.
106. Bouldin CM, Kimelman D. Cdc25 and the importance of G2 control: insights from developmental biology. *Cell Cycle* 2014, 13:2165–2171.
107. Edgar BA, Schubiger G. Parameters controlling transcriptional activation during early *Drosophila* development. *Cell* 1986, 44:871–877.
108. Newport J, Kirschner M. A major developmental transition in early *Xenopus* embryos: II. Control of the onset of transcription. *Cell* 1982, 30:687–696.
109. Newport J, Kirschner M. A major developmental transition in early *Xenopus* embryos: I. characterization and timing of cellular changes at the midblastula stage. *Cell* 1982, 30:675–686.
110. Kim SH, Li C, Maller JL. A maternal form of the phosphatase Cdc25A regulates early embryonic cell cycles in *Xenopus laevis*. *Dev Biol* 1999, 212:381–391.
111. Mata J, Curado S, Ephrussi A, Rorth P. Tribbles coordinates mitosis and morphogenesis in *Drosophila* by regulating string/CDC25 proteolysis. *Cell* 2000, 101:511–522.
112. Grosshans J, Wieschaus E. A genetic link between morphogenesis and cell division during formation of the ventral furrow in *Drosophila*. *Cell* 2000, 101:523–531.
113. Seher TC, Leptin M. Tribbles, a cell-cycle brake that coordinates proliferation and morphogenesis during *Drosophila* gastrulation. *Curr Biol* 2000, 10:623–629.